Camera tracking and qualitative airflow assessment of a two-turn erect spin

R. I. Hoff
rein.hoff@brunel.ac.uk
G. B. Gratton
guy.gratton@brunel.ac.uk
Brunel Flight Safety Laboratory
School of Engineering and Design
Brunel University
Uxbridge, UK

ABSTRACT

Motion and airflow during a two-turn erect spin of an aerobatic light aeroplane have been analysed. An alternative method, based upon camera tracking, has been used to capture the spin motion. A CAD model of the Slingsby Firefly was created using laser scanning. Formation flights with a helicopter have been flown and high-quality video and still imagery obtained. Camera tracking has produced data and unique illustrations of the spinning Slingsby. To further investigate the aerodynamic flow of a spinning aeroplane, full-scale, flow visualisation flights have been flown using wool tufts on wing, fuselage and empennage. Tufts indicate that a large vortex forms on the outside wing. The spanwise motion of this vortex has been studied and related to the spin motion. Furthermore, tufts on the horizontal tail indicate the presence of a leading edge vortex with the flow mainly in a spanwise outwards direction. The effects observed are clearly three dimensional and time dependent. Finally, it is discussed how this new knowledge does not correspond with the spin theories of the past.

Paper No. 3711. Manuscript received 5 April 2011, revised version received 26 September 2011, accepted 4 November 2011.

https://doi.org/10.1017/S0001924000007028 Published online by Cambridge University Press

NOMENCLATURE

b	wingspan
CAD	computer-aided design
CG	centre of gravity
F	fuselage area under the horizontal tail
L	length from CG to centroid of area F
L_2	length from CG to centroid of area R_2
R_2	rudder area under the horizontal tail
S	wing area
TDPF	tail damping power factor
α	angle-of-attack
β	angle-of-sideslip
2D	two-dimensional space
3D	three-dimensional space

1.0 INTRODUCTION

This research project was initiated as a result of challenges met during a flight test programme of the Piel Super Emeraude CP328, an amateur-built, single-engine low wing light aeroplane. During the initial flight test programme, the builder increased the size of the rudder to improve crosswind capability. With the aeroplane in final aero configuration and in preparation for spinning, a method was sought to alleviate the inherent risk of spin testing this aeroplane with its modified tail. It would be of great value for the flight test team to be able to predict if the aeroplane tail surfaces were of sufficient size to affect a spin recovery.

One such spin recovery prediction method that initially seemed very promising was the NASA tail damping power factor (TDPF). Considering the tail surface geometry, in particular the size of vertical surfaces and how they are placed in relation to the horizontal surfaces is the crux of this method. However, later wind-tunnel research by NASA led to a discounting of the TDPF method. These research results are not universally understood in the flight test community. For example, using TDPF as a risk mitigation tool was recommended in papers presented in 2006 at the European Symposium of the Society of Experimental Test Pilots[1,2]. Furthermore, the current UK Defence Standard[3] also encourages use of a similar spin recovery criterion, which includes an 'unshielded rudder volume coefficient'.

A limited spin test programme was completed for the Super Emeraude using a careful, incremental spin flight-testing approach. Spin recovery could be effected by using standard recovery controls (rudder full opposite the direction of spin, stick centrally moved forward until the spin stopped, controls centralised and the aeroplane pulled out of the resulting dive).

Although a limited spin test programme was successfully completed for the Super Emeraude, this clearly showed the need for more full-scale spin research. A spin research programme was initiated at the Brunel Flight Safety Laboratory and a Slingsby Firefly military trainer, with a configuration representative of the modern light aeroplane, was chosen as the research aeroplane.

Acknowledging that the spin is the most complex aeroplane motion, the first step in this research program was capturing the motion. A vision-based state estimation approach was chosen using camera tracking technology and video imagery of the spinning aeroplane 'shot' from a

https://doi.org/10.1017/S0001924000007028 Published online by Cambridge University Press

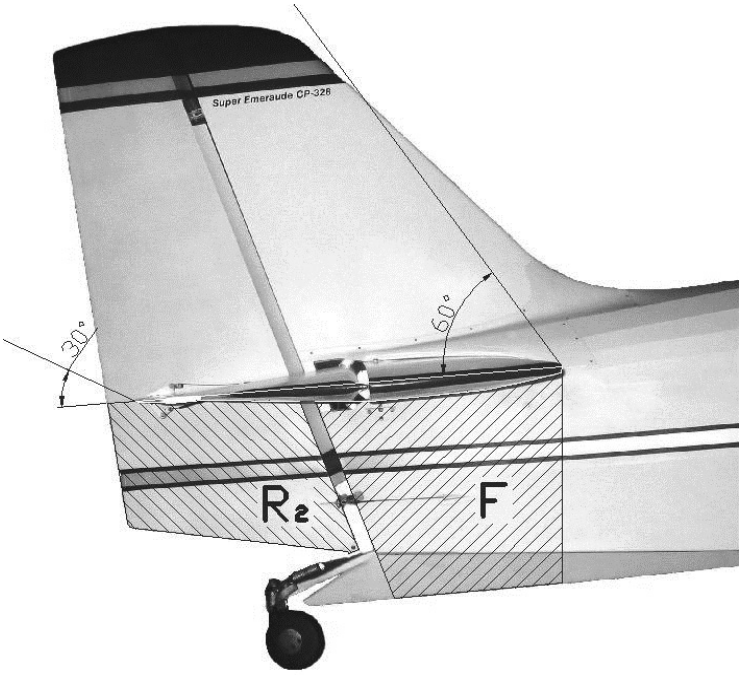


Figure 1. The unshielded areas under the horizontal tail of the Piel Super Emeraude.

helicopter chase aircraft. A CAD model of the research aeroplane was required for the camera tracking and was thus created using laser scanning. The next step was a qualitative assessment of the aerodynamic flow over wings and empennage using in-flight photographing of wool tufts. Finally, the observed aerodynamic flow was related to the motion of the spinning aeroplane.

2.0 BACKGROUND

The tail is believed to make the most important aerodynamic contribution to the nature of spin recovery. The rudder is the primary control for managing pro or anti spin yawing moments, so it is unsurprising that many researchers have concentrated upon tail design theories and guidelines. The first attempt to create such a design guideline was based upon wind tunnel results and created by RAE in the period 1934 to 1937[4]. These guidelines were further developed by NACA using further wind tunnel data. This approach allows for tail geometry, but also mass distribution and relative density of the aeroplane, and results in the term tail damping power Factor, or TDPF, which has been used since the 1930s as a guide to tail design for good spin recovery[5].

The TDPF criterion was implemented for the modified Super Emeraude. The unshielded areas believed to contribute to the 'damping of the spin' are shown in Fig. 1 and the TDPF given by:

$$TDPF = \frac{FL^2}{S(b/2)^2} \times \frac{R_2 L_2}{S(b/2)} \quad \ldots (1)$$

where F and R_2 are the unshielded areas under the horizontal tail as shown in Fig. 1, L the length

https://doi.org/10.1017/S0001924000007028 Published online by Cambridge University Press

from *CG* to the centroid of area *F*, L_2 the length from CG to the centroid of area R_2, *S* the wing area and finally *b* is wingspan.

Although the outcome was positive ('recovery by rudder alone'), and no problems encountered while spin flight-testing the Super Emeraude, this method seemed to be too simple for something as complex as the spin. A further literature review revealed that NASA had eventually discounted the TDPF criterion. NASA performed an investigation in the Langley spin tunnel on a 1:11 scale model of a research aeroplane, which represented a typical low-wing single engine, light general aviation aeroplane[6]. The tail assembly of the model was removable and nine different tail configurations were used. When correlating the results with the predictions from the tail design criterion, discrepancies were found. They concluded that TDPF: 'cannot be used to predict spin-recovery characteristics. However, certain principles implicit in the criterion are still valid and should be considered when designing a tail configuration for spin recovery.' After additional wind tunnel research by the same organisation in 1989, they stated that the TDPF criterion: 'can give misleading results and should never be used'[7]. The results from this study showed that the assumptions made when the TDPF criterion was first conceived are wrong. The assumption made for the TDPF criterion was that the horizontal tail causes a wake that effectively shields the vertical tail surfaces. Furthermore, it was assumed that the vertical tail and the rudder in the 'free air stream would be effective for recovery'. This study on the other hand showed that damping is contributed by[7]: 'the inboard side of the fuselage and vertical tail, as well as by the fuselage area on the outboard side under the horizontal tail.'

3.0 CAMERA TRACKING: CAPTURING THE SPIN MOTION

To be able to study the spin motion of the aeroplane in adequate detail, quantitative data is required. Of particular interest are the angles between the aeroplane body axes and the relative wind such as the angle-of-attack and sideslip. Furthermore, the components of the angular velocity vector, rate of roll, pitch and yaw, are essential data. The classic approach to capture the spin motion of a given aeroplane is by measurement of several parameters using on-board instrumentation. The aeroplane instrumentation will typically be air-data sensors mounted on a boom to measure flow angles and true airspeed ahead of the wing and a solid-state gyro package to measure accelerations along the body axes. In addition the control surface positions and forces might be recorded. The key parameters describing the spin motion are then plotted as time histories. For example NASA, as part of a comprehensive stall/spin research programme, has conducted several full-scale experimental spin investigations using general aviation aeroplanes and published detailed time histories[8-10].

However, this classic approach will necessarily require a properly instrumented aeroplane. Instrumenting an aeroplane is expensive and it will also alter the aeroplane modification state. There will also always be airworthiness implications when instrumenting any aeroplane. Furthermore, the well known challenge in experimental physics: how to measure a system without influencing it, is also applicable to the aeroplane spin. When instrumenting a light general aviation aeroplane, the modification might change both of the 'spin fundamentals': inertia and aerodynamics. Whilst flight testing the Lancair Columbia 400[11], the aerodynamic effect of the boom was found to be equivalent to a slight rudder deflection. Furthermore, it was found that the boom degraded the spin recovery characteristics.

In this research programme an alternative method has been developed to capture the spin motion. Finding an alternative approach was mainly motivated due to cost involved in instrumenting the research aeroplane. In addition, the aeroplane chosen for the research programme

https://doi.org/10.1017/S0001924000007028 Published online by Cambridge University Press

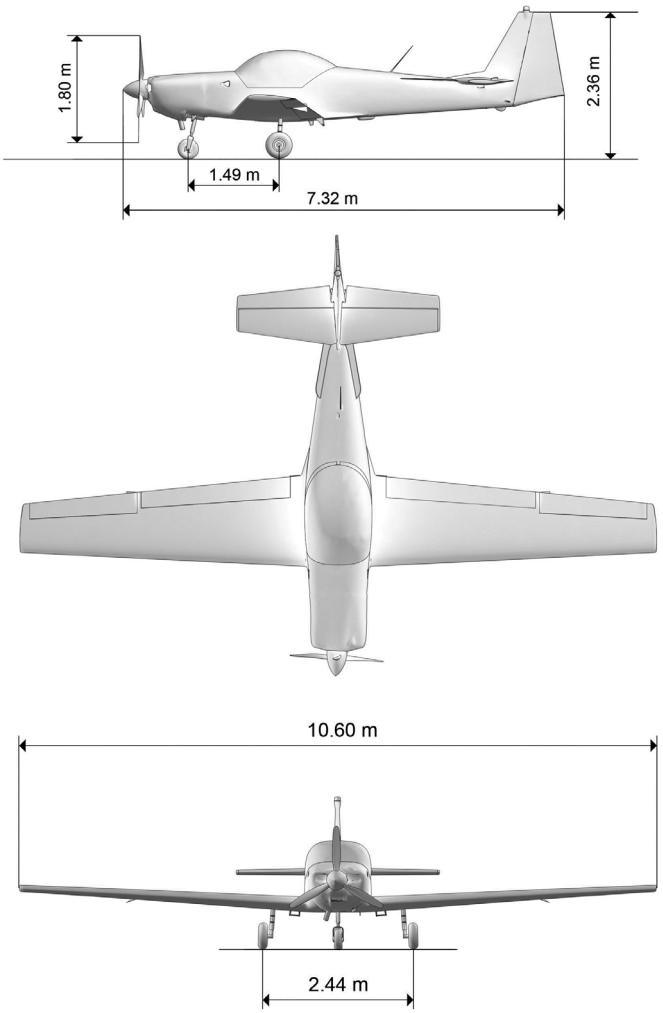


Figure 2. A three-view of the Slingsby Firefly T67M200.

was a certified aeroplane and changing the airworthiness status would have been very difficult. This method (as outlined below) is based upon camera tracking. The main resources in this camera tracking are a complete aeroplane CAD model and high quality video imagery of the motion. The CAD model was required to go from the 2D video imagery to a 3D model of the spin motion.

3.1 The research aeroplane and the two-turn spin

The aeroplane chosen for this research programme was a Slingsby T67M200 Firefly. This particular aeroplane is aerobatic category and representative of the typical single-engine military type trainer, with fixed gear and a 200 horsepower engine. A three-view of the Slingsby model used is shown in Fig. 2 and details are listed in Table 1 (data from the Slingsby T67M200 Pilots Notes[12]).

https://doi.org/10.1017/S0001924000007028 Published online by Cambridge University Press

Table 1
Slingsby Firefly T67M200 general data[12]

Fuselage:	
Overall length (m)	7·323
Overall height (m)	2·36
Wing:	
Span (m)	10·6
Surface area (m^2)	12·6
Dihedral	3°30′
Incidence at root	3°
Incidence at tip	0°20′
Root section	NACA 23 015
Tip section	NACA 23 013
Area of one aileron (m^2)	0·62
Horizontal tail:	
Fixed surface area (m^2)	1·65
Elevator surface area (m^2)	0·99
Vertical tail:	
Fin surface area (m^2)	0·8
Rudder surface area (m^2)	0·81

The spin evaluated was the erect, idle power two-turn spin used in a typical aerobatic training curriculum. The two-turn spin was performed in the Slingsby Firefly using the following steps:

1. A visual reference was chosen on the ground and in front of the aeroplane. This reference was used to count the number of turns.
2. The stall was entered from level flight, with engine set to idle power.
3. Speed was reduced towards stall speed (deceleration rate 1kt/sec). At just before (1kt) the indicated stall speed, spin controls were set simultaneously. If spinning to the left, spin controls were full left rudder and full aft stick with ailerons centred.
4. The aeroplane entered the spin, and turns counted when passing the reference mark chosen on the ground.
5. At two turns, spin recovery controls were set. For a left turn spin, the rudder was set from full left to full right (rudder reversed). After the rudder was set full opposite the turn direction, the stick was centrally moved forward until the spin stopped.
6. Depending on the actual mass properties, atmospheric conditions and pilot recovery technique, the spin in this aeroplane normally stopped after 0·8 to 1·5 additional turns. The controls were then centralised and the aeroplane pulled out of the resulting dive.

3.2 The creation of the aeroplane CAD model

A complete and accurate CAD model was required for camera tracking. Targets on the spinning aeroplane, as shown on the video imagery, were mapped onto the 3D model. The approach chosen to create this model was laser scanning using a Leica HDS scanner[13]. The laser scanning process resulted in an ‘as-built’ digital 3D model of the actual aeroplane used in this spin research programme.

https://doi.org/10.1017/S0001924000007028 Published online by Cambridge University Press

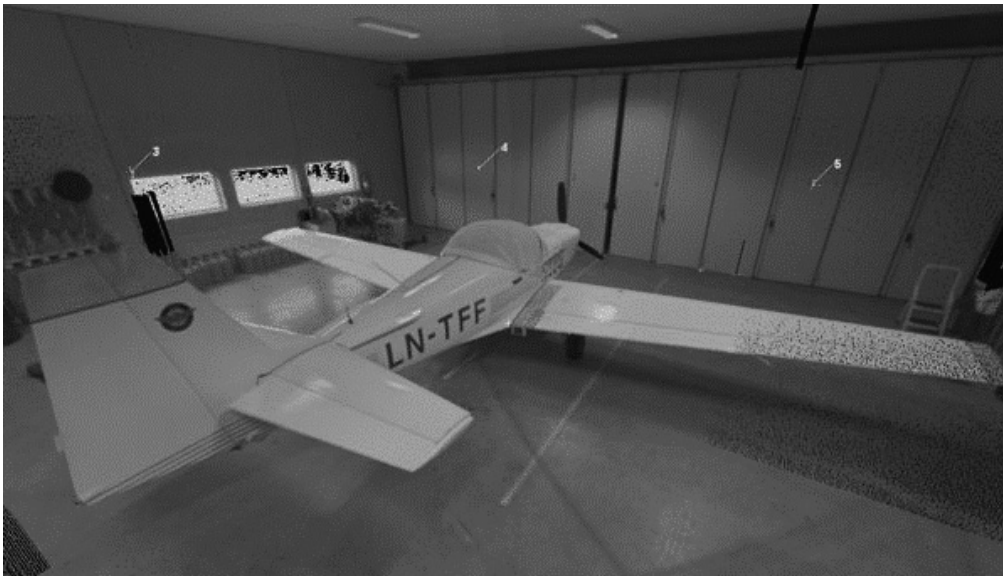


Figure 3. The point-cloud of the Slingsby Firefly. Note the laser scan targets on the walls.

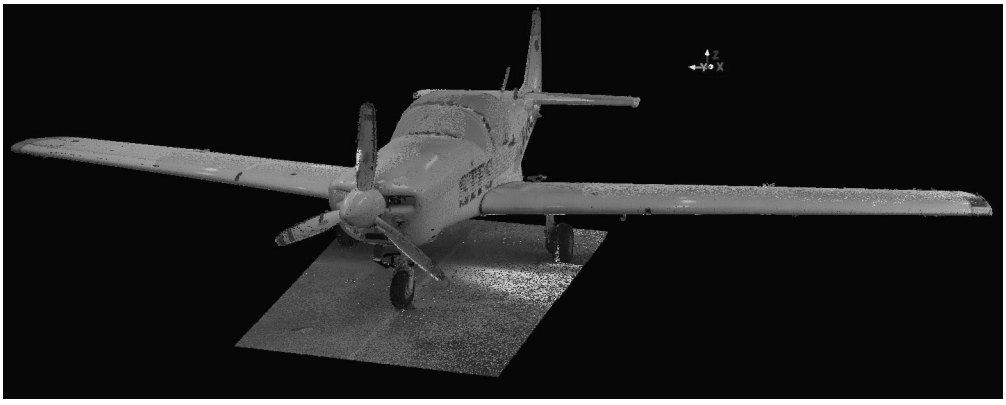


Figure 4. The Slingsby Firefly point-cloud before the meshing procedure.

The Slingsby was scanned in the hangar, using nine different laser scanner positions around, above and under the aeroplane. Laser scan targets, used to merge the scans, were placed on the walls and on various stands in the hangar. In addition, colour photos were taken from each scan position. These colour photos were used to overlay colour on the 3D point-cloud. A total of 29·9million data points were collected on the aeroplane. The nine scans were merged into one point-cloud. Figure 3 shows this point-cloud from one of the nine scan positions.

After post-scan data processing using Leica Cyclone[14] software, a meshing procedure was applied to go from a point-cloud to a usable 3D CAD model. The point-cloud was thus imported into the 3Dreshaper[15] software application. The aim of the meshing procedure was to eliminate incoherent points, filter and smooth to reduce the model. It was a challenge to find the right meshing properties and most of the meshing had to be edited manually. Figure 4 shows the point-cloud before the meshing procedure and Fig. 5 shows the CAD model after the meshing procedure.

https://doi.org/10.1017/S0001924000007028 Published online by Cambridge University Press

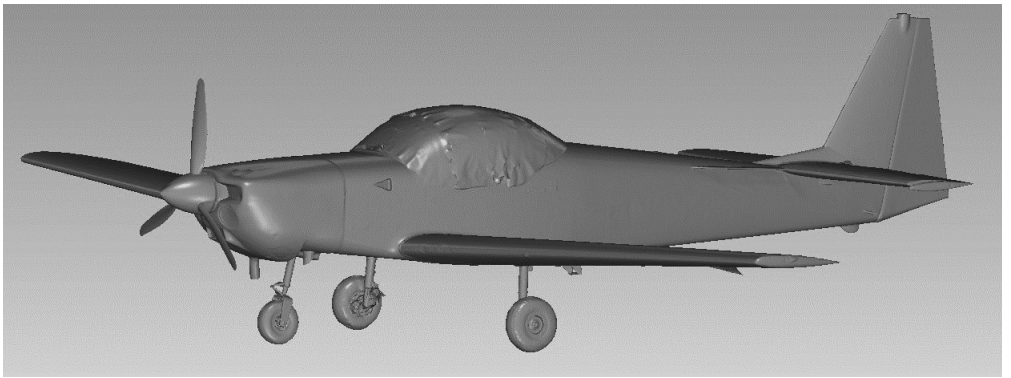


Figure 5. The Slingsby Firefly after the meshing procedure.



Figure 6. The camera installation in the helicopter.



Figure 7. The flight position of the camera operator.

3.3 Obtaining high quality video imagery of the two-turn spin

Having created a CAD model of the research aeroplane, the next step was to obtain high quality video imagery of the two-turn spin. Due to the near vertical high-rate descent, it was difficult to capture the spin from a chase aircraft. In the Slingsby Pilot Notes[12], the height loss is given as 250ft per turn, plus 500ft for recovery. The approach chosen was to use a helicopter as chase aircraft. The helicopter is a stable camera platform and high-end camera rig installations are available. In addition, the helicopter can enter an autorotation with a resulting high-rate of descent (approx 1,500-1,800ft/min.). However, even if the helicopter is autorotating, it cannot match the rate of descent of a spinning aeroplane (estimated to be twice the rate of the helicopter from entry to second turn, increasing as the spin develops).

The helicopter type used as a chase aircraft was a Eurocopter AS350 BA. The left door was removed and a Panasonic AG-HPX500[16] camera (with 16 × 6·3 mm optics) was mounted in a special purpose rig. The camera was gyro stabilised using three Kenyon Labs KS-8[16] gyros. This camera installation enabled the camera operator a clear view of the spinning aeroplane at all times. The camera installation is shown in Fig. 6 and the flight position of the camera operator is shown in Fig. 7. In addition, a Pentax K20D[18] (with a 50-135mm f/2.8 lens) still photo camera was used with a photographer taking photos from the left front seat.

Due to the elevated risk of formation flight a detailed formation procedure was used. A pre-flight briefing was held with all crewmembers present and the applicable air traffic control unit was contacted and briefed on the flight and formation procedure.

https://doi.org/10.1017/S0001924000007028 Published online by Cambridge University Press



Figure 8. Left spin entry (just over ½ turn) 'shot' from the helicopter.



Figure 9. The Slingsby Firefly about to complete one-turn in the spin.

The helicopter entered holding at a pre-determined rendezvous point in the designated block of airspace. The aeroplane intercepted the helicopter and joined up in line abreast formation. A beach line was used as the ground reference for the spin. When the helicopter was safely in position and the camera operator confirmed an acceptable camera angle, a radio call was made from the helicopter to continue as planned.

The aeroplane was put into a two-turn spin to the left, with the helicopter positioned to the right, behind and slightly below the aeroplane at spin entry position. As the aeroplane reduced speed to enter the spin, the helicopter reduced speed towards 40kt indicated airspeed. When the Slingsby entered the left spin, the helicopter pilot initiated autorotation. It was apparent immediately that the rate of decent of the Slingsby in the spin was greater than that of the helicopter in autorotation.

When the aeroplane had completed one turn, the helicopter pilot turned slightly left to enable the camera operator to follow the aeroplane in the spin. The indicated airspeed in the helicopter during autorotation was approx. 40kt. As the aeroplane recovered from the spin, the helicopter recovered from the autorotation.

High quality video and still imagery of the left two-turn erect spin were obtained. Examples of the very high quality images 'shot' from the helicopter are shown in Figs 8 and 9. In Fig. 8 the aeroplane has entered the left turn spin, completed just over ½ turn over the beach line, and full left rudder and full elevator up (aft stick) is set. The aeroplane was just about to complete the one-turn in Fig. 9 and will in the next split second roll and yaw further to the left.

3.4 Camera tracking procedure

The final step in the spin motion capture process was, using the video imagery 'shot' from the helicopter, to match targets on the spinning aeroplane to the CAD model using SynthEyes[19] camera tracking software. Several targets were selected on the airframe, e.g. the tip and bottom of the vertical tail, wing- and horizontal tail tips and the centre of the wheels. As the aeroplane rotates in view, new additional points are established. The raw 3D animation from SynthEyes, describing the motion of the aeroplane in 3D, was then imported into Autodesk 3D max[20] software package for further processing.

https://doi.org/10.1017/S0001924000007028 Published online by Cambridge University Press

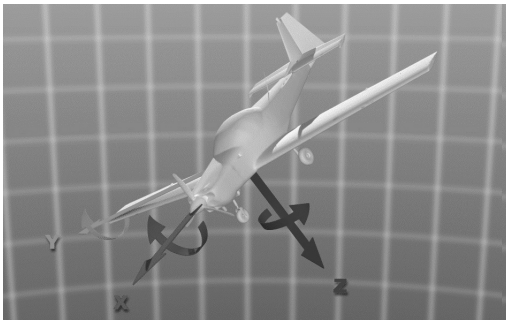


Figure 10. Spin motion frozen in the three-dimensional space and view rotated.

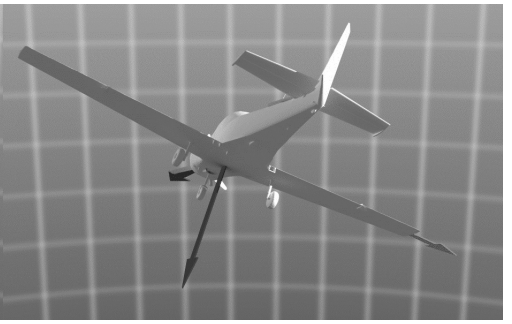


Figure 11. Another view angle of the same spin position as in Fig. 9.

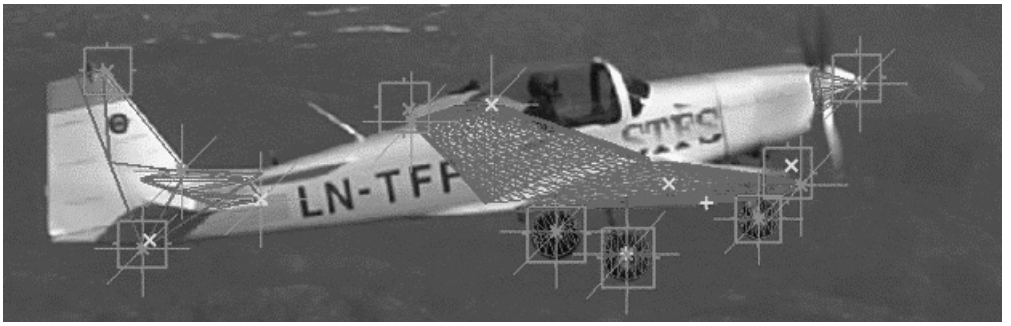


Figure 12. A screenshot from SynthEyes[19] showing points on aeroplane with geometry overlay from the CAD model and points in the background.

The result from this preliminary camera tracking test was promising. The CAD model spinning in a digital three dimensional space could replace the Slingsby spinning in the movie. The spin motion can be frozen at any time and the view rotated 360° in any direction. Screenshots from the spin animation are shown in Figs 10 and 11. The spin position frozen is the same as shown in Fig. 9 (just before one-turn in the spin), but the view angle is rotated and the aeroplane shown from two different angles.

Looking at the movie first and then the animated Slingsby spin second, it appeared to be the same motion. For illustration purposes this camera tracking seemed to be a perfect match. However, when trying to quantify the data (e.g. estimating angle of attack and sideslip), it became clear that the animated motion was not perfect. The rotational motion of the aeroplane seemed to be reasonable; however, the translational motion was rather erratic. The reason for this lack of quality was believed to be due to the motion of the camera in the helicopter. Thus, another formation flight was flown were the aim was to track both the spinning aeroplane and the camera motion. To be able to track the camera motion, the Slingsby was still spinning over the beach line, but this time in the other direction with land instead of sea in the background. In addition to points on the aeroplane, tracking points were established on the terrain in the background. A screenshot from SynthEyes[19], showing points on aeroplane with geometry overlay from the CAD model and points in the background, is shown in Fig. 12. Ideally, a dual tracking of both aeroplane and camera will result in the 'true' spin motion. However, tracking the camera turned out to be a real challenge. First, the helicopter itself is not in steady motion during the

https://doi.org/10.1017/S0001924000007028 Published online by Cambridge University Press

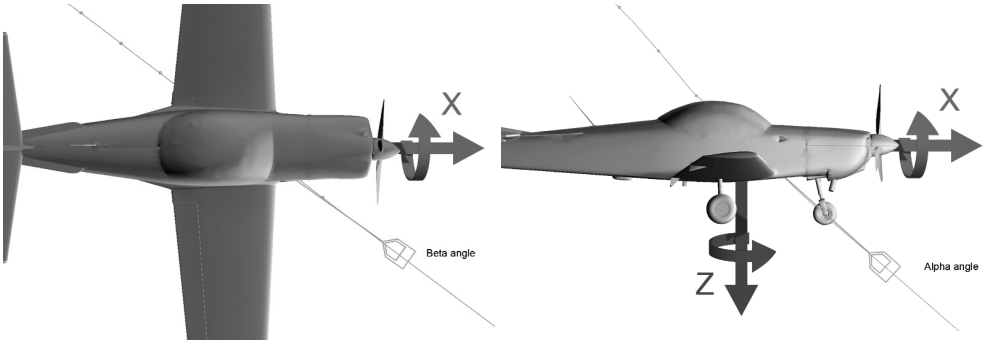


Figure 13. Estimated angle-of-attack (Alpha) and sideslip (Beta) were measured every fifth frame.

autorotation. Secondly, the camera operator is constantly adjusting the gyro stabilised camera angle in order to capture the spinning Slingsby.

The result from the second flight was successful in the sense that the aeroplane trackline (the path of the CG in 3D) was established. But due to the complex helicopter camera motion the initial conditions was not established and post processing of data was required. A speed reduction scheme (from 59 to 40kt in four seconds and then linear reduction to 17kt at end of tracking) was imposed for the camera motion and the trackline was aligned to direction of flight. The rotational motion was unaltered. The initial angle-of-attack (Alpha) at spin entry was estimated at 15°. Having established the trackline in 3D, estimated Alpha (α) and Beta (β) was recorded every fifth frame (Fig. 13). Alpha angle was estimated to the angle between the *X*-axis and the trackline component in the *XZ*-plane, and likewise Beta angle the angle between the *X*-axis and the trackline component in the *XY*-plane.

The advantage of using this method to create illustrations for flight training or academic use is clear. The spin motion, which is truly the most complex of the aeroplane motions, can be frozen at any time and the view rotated 360° around any axis. The angles and how they relate in the three dimensional space can be studied from all sides. Fig. 14 shows the final result of an illustration created to visualise the spin motion. Three spin positions, where the second position is the same as shown in Figs 9, 10 and 11 above, are frozen on the trackline.

Ideally, camera tracking is a 'what-you-see-is-what-it-is' approach to flight testing. If this alternative method is successful, advantages are that there will be no calibrating issues with complex on-board instruments. In a university environment, having access to special purpose full-scale aeroplanes is not common. Therefore, the cost and time involved for instrumentation can be a hindrance for full scale aeroplane flight testing. With the use of camera tracking, data can be obtained by using aeroplanes available for rent for a limited time. The cost driving factors will be the creation of a CAD model, the chase aircraft and the required camera equipment. For this research programme a helicopter was used, which is a rather expensive solution for chase aircraft. However, the cost involved with helicopter hire for a day or two, is small compared to the costs involved with having a special purpose and instrumented aeroplane available. When studying other motions than the spin, not involving such a high rate of descent, less expensive chase aircraft might be used.

https://doi.org/10.1017/S0001924000007028 Published online by Cambridge University Press

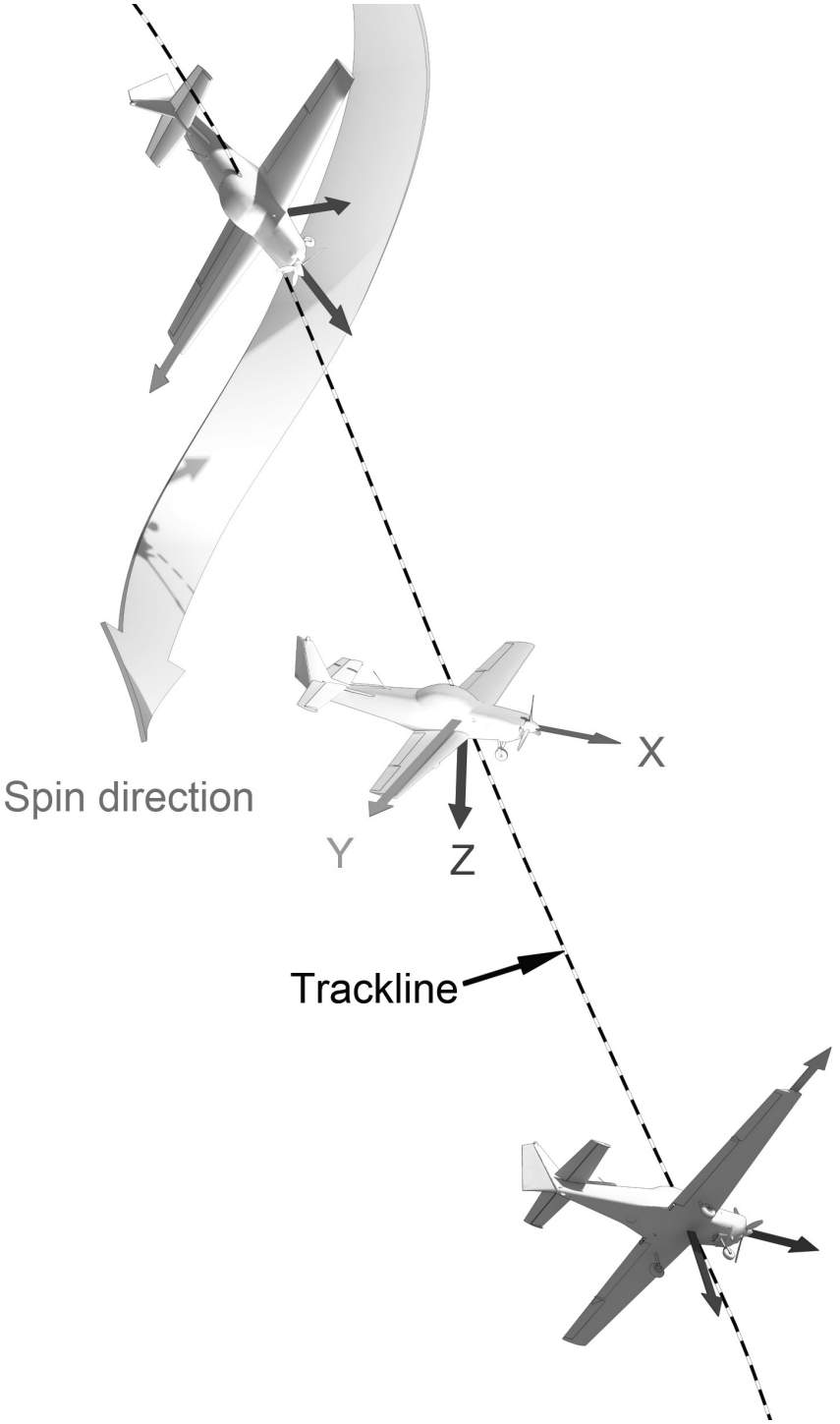


Figure 14. An illustration showing three spin positions frozen on the trackline.
The second position is the same as shown in Figs 9, 10 and 11.

https://doi.org/10.1017/S0001924000007028 Published online by Cambridge University Press

4.0 A QUALITATIVE ASSESSMENT OF THE AERODYNAMIC FLOW OVER WINGS AND EMPENNAGE

A qualitative assessment of the aerodynamic flow over wings and empennage of the spinning Slingsby was carried out using in-flight photographing of wool tufts. This technique for studying the flow on a spinning aeroplane has been used many times before. As early as 1932, Jones and Haslam[21] studied the airflow over the wings and tail by using wool tufts on a spinning Atlas biplane. The turbulent nature of the flow was clearly shown. About four seconds after the start of the spin the flow over the outside top wing was mainly irregular, but there was also areas with unsteady streamline and also reversed flow. The outside lower wing was mainly streamline with irregular flow on the inner section. However, the inside upper wing was irregular and the bottom wing had very marked and steady reversed flow. In a more recent research program by Brown *et al*[22] at the National Research Council in Canada, the wings of a Harvard Mark 4 were tufted with wool tufts and the airflow studied while spinning by using video imagery. They describe the airflow in more detail, e.g. the authors' statement regarding the flow on the outside wing (in this case the left wing in a erect, right turn spin): 'Although some large-scale eddy (LSE) coherence was evident at times (…), it is non-stationary. This is indicative of the temporal formation of LSE in the separated flow, followed by downstream eddy convection'.

Furthermore, Brown *et al* also describe the airflow on the inside wing: '… the tuft patterns appeared to be dominantly arranged about a ¼ chord vortex, of clockwise-rotational sense, located at the mid-span position. Video imagery tended to suggest the vortex was frozen, or quasi-stationary, with respect to the wing, rather than being formed and convected downstream.'

It is worthwhile to study in detail the aerodynamic flow on a more modern aeroplane design such as the Slingsby Firefly. Furthermore, it is of interest to investigate the shielding of the tail effect, as this is the main assumption behind the tail design criterion[5]. The wake from the tail plane is assumed to be in the region bounded by a 60° line from the leading edge and a 30° line from the trailing edge (as shown in Fig. 1).

4.1 Experimental setup details

Wool tufts of approximately 15cm length were placed along the wings and both horizontal and vertical tail. In addition, tufts were placed on the left aft fuselage side. Wool tufts illustrate the principal airflow direction at the aerodynamic surface and indicate areas of separated flow. The tufts placed on the Slingsby research aeroplane can be seen in Fig. 15.

Several on-board cameras were used to capture the tufts on the spinning Slingsby. The principal camera positions were on the left wingtip, inside the cockpit shooting movie of the tufts on the wing through the transparent Perspex canopy and on top of the aft fuselage. Due to the requirement that the camera had to be small and self-contained, several 'action type' cameras were initially tried. The results from these tests were not promising, and in addition to poor movie quality there were reliability problems with the 'action type' cameras used. Therefore, to produce better quality video imagery, camcorder cameras were used instead. The mounting arrangement on the wing tip was inspired by sport parachute equipment, using Velcro fastener, a special purpose remote control and safety wire. The camcorder used on the wing tip was a Sony HDR-CX105[23] and a JVC Everio G[24] was used inside the cockpit. On the aft fuselage a Muvi Micro Camcorder[25] (mass approx. 50g and dimensions 55 × 28 × 22mm) was used to capture the tufts on the horizontal tail. This camera was mounted using a double set of mounts for redundancy.

https://doi.org/10.1017/S0001924000007028 Published online by Cambridge University Press



Figure 15. Four movies were synchronised and shown together in the same image. The Slingsby has completed one-turn in the spin at four seconds and ten frames (the spin entry was at 0 second 20 frames).

In addition to the on-board cameras, the helicopter had both a high-end movie camera rig and a still photo camera operator in the front seat, as described in Section 3.3. The video and still imagery obtained from the helicopter were high quality and well suited for post-flight analysis.

To aid the analysis, four movies were synchronised and shown together in the same image. To enter the spin, the controls are set to full deflection. This setting of pro-spin control positions was used to synchronise the movies. In addition, it was possible to crosscheck the synchronisation by using the fact that momentarily one of the cameras was shooting another camera. For example, the helicopter was shown in some frames from the wing tip camera. When the helicopter disappears from view, the wing tip camera itself should at the same instant disappear from view in the helicopter camera frame. The camera frame rate was 25 frames per second. The exception was the Muvi Micro Camcorder, which had a rate of 20 frames per second. Therefore, it was a challenge to synchronise the movie from the Muvi Micro camera. The first frame in one second was synchronised and then the remaining 19 frames are slightly out of sync (+/–15ms).

For a two-turn spin, (two-turns + normally one-turn in recovery), approx. 320 images were therefore generated. One of these synchronised images is shown in Fig. 15. The 'time code' shown in the middle of the image is: spin number (several two-turn spins were flown during each flight) : minute : second : frame number (25 frames per second).

4.2 Flow over the wings of the spinning aeroplane

In order to describe the flow, as indicated by observing tufts on the wing, some definitions will now be made. The inside wing is the same side as the spin direction, e.g. in a spin to the left, the inside wing will be the left wing and the outside wing will be the right wing. Spanwise flow is either outwards (direction from wing root to tip) or inwards (direction from wing tip to root). Streamline flow is from leading edge of the wing towards the trailing edge. Conversely, reverse

https://doi.org/10.1017/S0001924000007028 Published online by Cambridge University Press

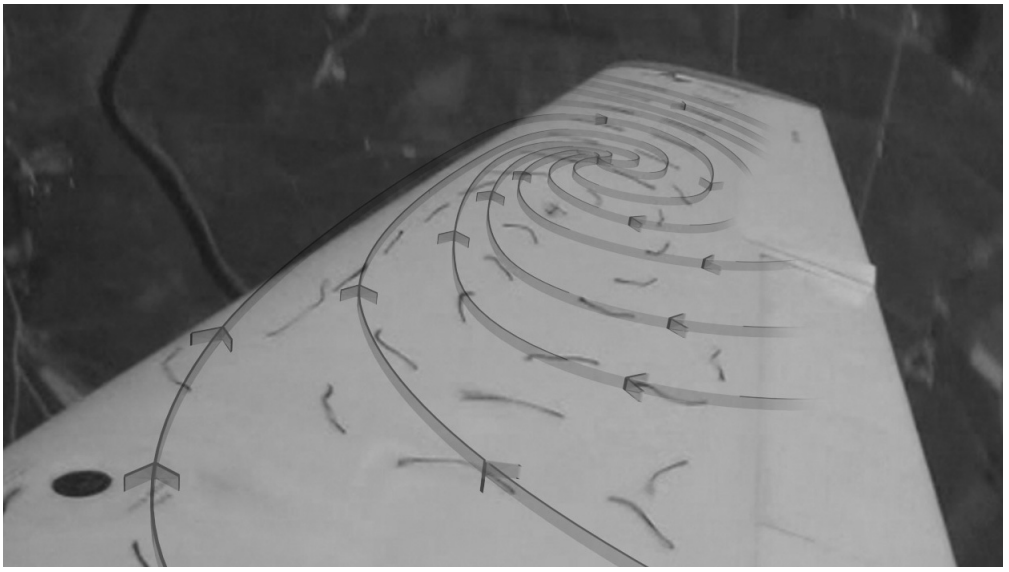


Figure 16. A large vortex forms on the outside wing as indicated by the wool tufts. The lines are drawn to illustrate how the shape of the vortex might be and arrows indicate flow direction.

flow is in the opposite direction (from trailing edge to leading edge). Unsteady streamline is typically used for the case where flow is mainly in the streamline direction, but the flow has separated and is clearly turbulent. In the case of irregular flow, no principal direction of the flow is indicated and the tufts have no pattern of movement (erratic motion).

4.2.1 Spin entry and first turn

Considering now the outside wing in a left spin. As the elevator was deflected trailing edge up for the spin entry, unsteady streamline flow was observed at the trailing edge of the wing root. From the spin entry point, where full elevator up position was set, irregular flow had moved from the trailing edge and reached the leading edge of the wing in eight frames. This only applied to the inner 2/3 section of the wing (from the wing root), and thus the flow was still attached (streamline) on the outer 1/3 section of the wing. At the point on the wing where the flap meets the aileron, a vortex flow structure was observed. This vortex structure was placed in the area where the flow transitions from irregular to streamline. When the Slingsby had rotated to a point where the wings were 90° to the horizon, the flow returned to streamline over the entire wing. The flow was streamline for the next 90° of rotation to the ½ turn point.

After the ½ turn point, a vortex formed and moved from the wing root (spanwise outwards). The rotational flow was clearly observed and it was a large vortex in the sense that its diameter seemed to be comparable to the wing chord (Fig. 16). At just past the ¾ turn, the rotational flow was most apparent and the vortex core observed at the approx. 1/3 chord position (Fig. 17). The flow behind the vortex was in the spanwise outwards direction. At one-turn the flow on the wing was predominantly spanwise outwards with a 90-degree turn towards the tip, leaving the three outer row tufts in the streamline direction (Fig. 15).

The tufts indicate a ‘twin peak’ in alpha during the first spin turn. The first peak is when the full spin controls are set. Then the angle-of-attack is apparently reduced, with streamline flow

https://doi.org/10.1017/S0001924000007028 Published online by Cambridge University Press



Figure 17. Tufts on the wing at just past the ¾ turn in a left hand spin. The vortex on the outside (right) wing is clearly seen where the flap meets the aileron. The vortex core is at the approx. 1/3 chord position.



Figure 18. At the two-turn point, spanwise outwards flow was clearly apparent on the outside wing. Only the outer rows of tufts are streamline. Irregular flow can be seen on the inside wing.

over the entire outside wing, before increasing again from the ½ turn to the one-turn. This is consistent with alpha time histories of other spinning aeroplanes, e.g. published data from the NASA general aviation research programme[8-10], where this twin peak in alpha during the first turn is clearly apparent.

The same technique was used to study the inside wing, but with the camera mounted on the right hand side, a right hand two-turn spin was naturally used. From spin entry, reverse flow develops, starting at the trailing edge and after ten frames from spin entry the reverse flow has moved to the leading edge, thus covering the entire wing. The flow on the inside wing during the first turn is best described as a mix of reverse and irregular. On many frames the reverse flow is apparent. However, studying one tuft from frame to frame it can be observed that the direction might change from reverse to streamline in two frames.

4.2.2 Second turn and recovery

First, we will again consider the outside wing in a left spin. From the one-turn and then ten more frames, the vortex rolled back (inwards) so that the outer seven rows of tufts were streamline. At 1·5 turns the vortex moved outwards again, and four rows of tufts were streamline. The spanwise outwards flow was clearly apparent at the two-turn point, and only one row of tufts were streamline (Fig. 18).

The spin recovery controls are set at the two-turn point. Rudder is reversed in seven frames and after six more frames the elevator starts to move. From this instant the vortex rolled inwards. One row at the time, from the wing tip towards to root, became streamline. The rate is such that after ½ turn in recovery the outer two rows are streamline and when the aeroplane had completed one full turn in recovery all of the outside wing tufts indicated streamline flow (Fig. 19).

https://doi.org/10.1017/S0001924000007028 Published online by Cambridge University Press



Figure 19. The aeroplane just before completing one turn with recovery controls set (the third turn from spin entry, left hand spin). All of the outside wing tufts indicate streamline flow. Flow on inside wing was still irregular at this point.

For the inside wing, the flow is best described as irregular. One tuft would typically rotate 90° in one frame. Mostly, no clear pattern was seen over the entire wing. This can be observed in Fig. 16, with tufts indicating several directions over the inside wing. However, at 1·5 turn and for a period of 11 frames the main direction of the flow can be described as reversed. From the

https://doi.org/10.1017/S0001924000007028 Published online by Cambridge University Press

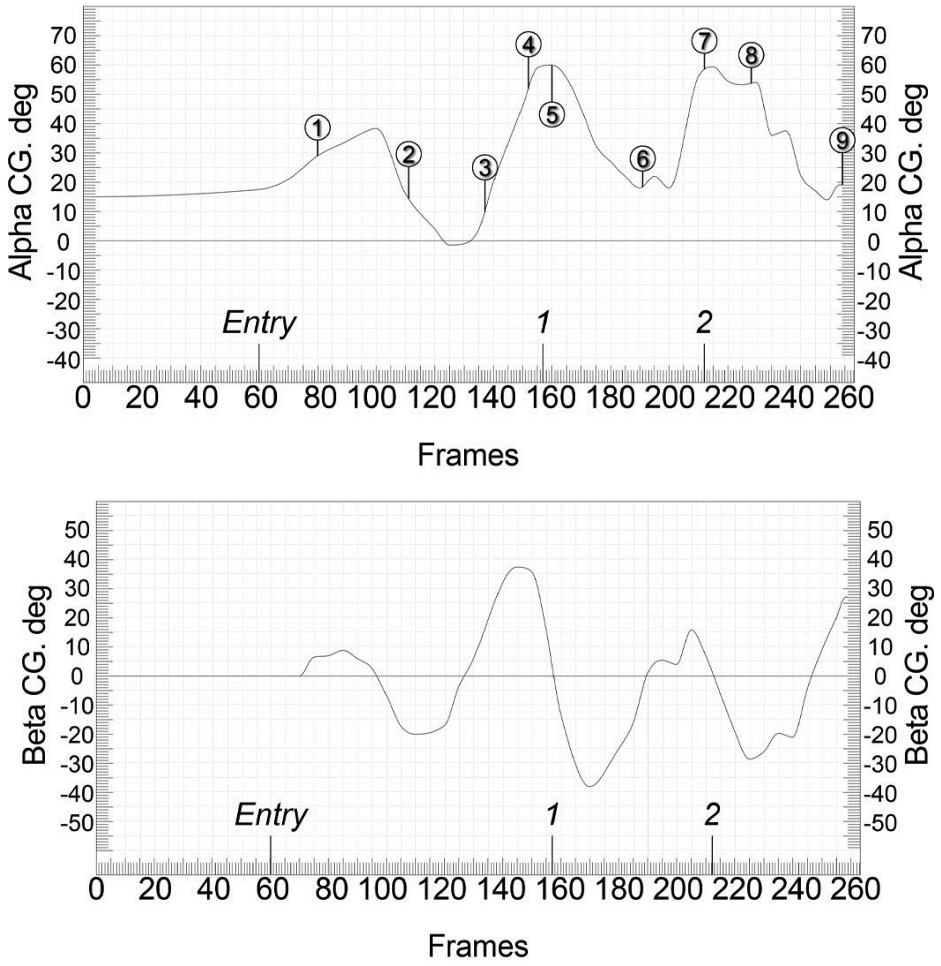


Figure 20. Alpha and Beta estimated using camera tracking. The numbers marked on the alpha graph correspond to the illustrations in Fig. 21.

point where spin recovery controls were set to just before recovery was complete (rotation ceased), the flow remained irregular (Fig. 19). One frame before rotation stops, the flow over the entire inside wing was streamline. The transition from irregular to streamline commenced 6 frames before recovery, and developed from root to tip, indicating a gradual decrease in angle-of-attack towards the wing tip.

The movement of the vortex on the outside wing (as described in this and previous section), have been illustrated, related to the estimated Alpha angle and shown together with the Slingsby position in the spin. The estimated Alpha and Beta angles have been plotted and are shown in Fig. 20. The corresponding slides are shown in Fig. 21.

https://doi.org/10.1017/S0001924000007028 Published online by Cambridge University Press

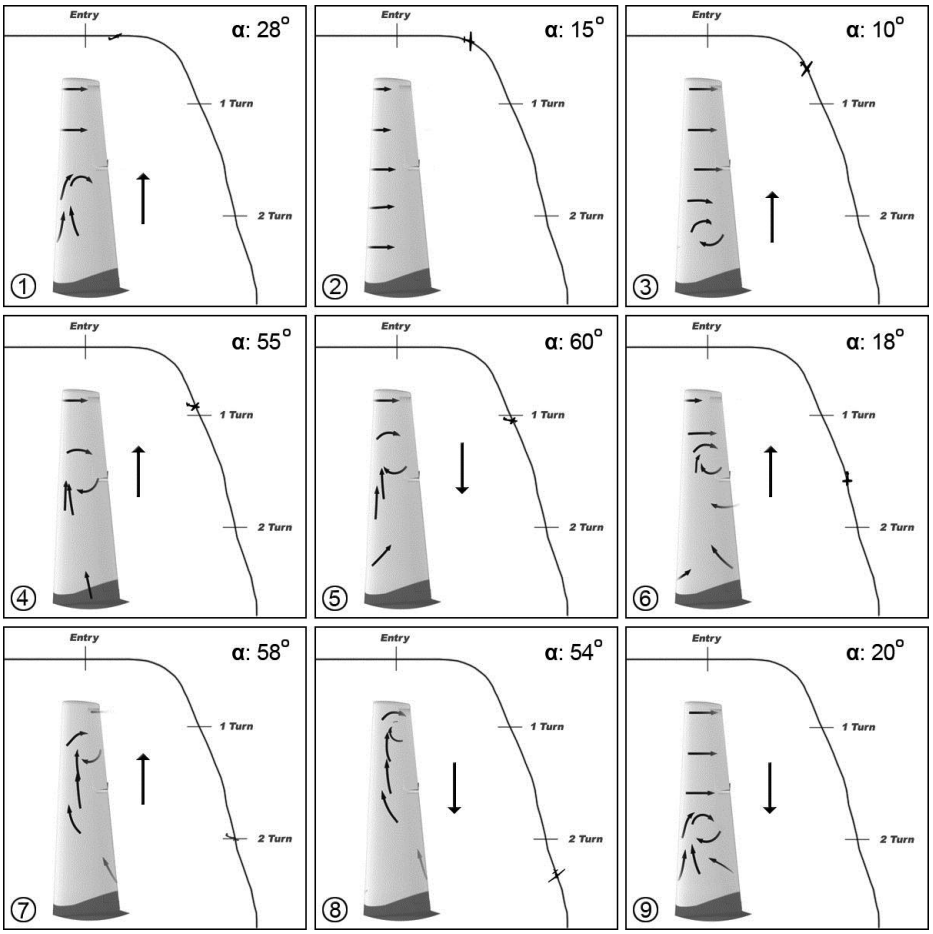


Figure 21. The vortex on the outside wing, shown together with the spin position and estimated Alpha (α). The miniature aeroplane is shown on the trackline. The arrows on the wing show the direction of airflow as indicated by the tufts. The arrow behind the wing indicates the direction of vortex movement on the wing. The numbers on each slide correspond with the estimated Alpha graph in Fig. 20.

4.3 Flow across the tail and aft fuselage

As the aeroplane was pitched up, but just before the controls were fully set for spin entry, the tufts at the inside fuselage indicated unsteady streamline flow. At entry, the flow on the inside vertical tail was unsteady streamline but deflected approximately 20° upward above the horizontal tail and deflected downwards below. After 15 frames the flow became irregular at inside fuselage and vertical tail.

After an additional seven frames, reversed flow was observed at the vertical tail, with the tufts pointing straight out from the leading edge of the vertical fin. This indicates the presence of a vortex at the tail. When the aeroplane has rotated to a point where the wings are 90° to the horizon, the flow at the tail is irregular, but direction is mainly in the streamline direction. Reverse flow, or rather highly irregular flow, was again apparent after the Slingsby had passed

https://doi.org/10.1017/S0001924000007028 Published online by Cambridge University Press

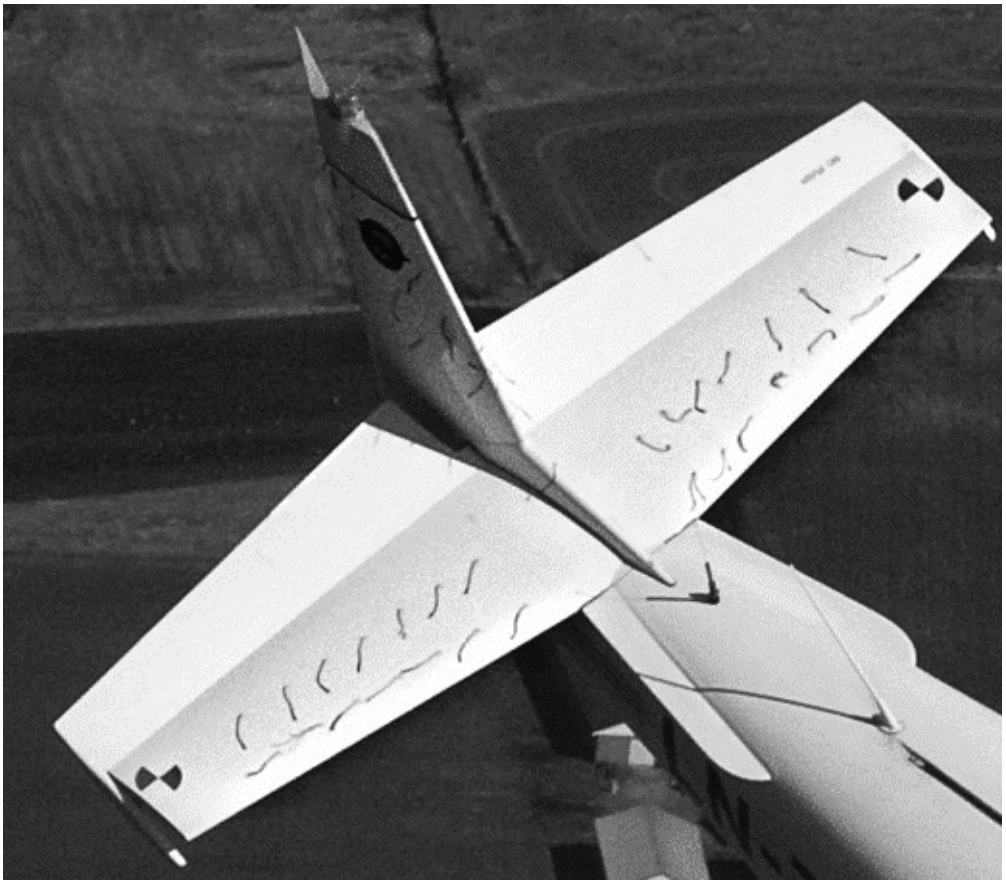


Figure 22. The tufts on top of the stabilisator indicate the presence of a leading edge vortex.

the ½ turn. This indicates that there might be a connection between the vortex forming on the outside wing and the irregular flow observed on the vertical tail.

The flow at the inside fuselage is irregular, however one flow direction seemed to be more dominant than the other, and that is 90° to the fuselage streamline direction. This indicates a rotational flow around the fuselage with a right angle to the spin strake and horizontal tail. Just before the spin recovery is complete (eight frames before rotation ceased), the flow at both inside fuselage and vertical tail was again streamline.

Observing the tufts on the outside fuselage and vertical tail, the flow seemed to be similar to that described above for the inside. Again, the dominant flow direction at the fuselage was straight up. One exception is the flow under the horizontal tail, which appeared to be either unsteady streamline or deflected approx. 30° downward. This difference in flow condition, from the inside to the outside, might correspond with the results from the wind tunnel investigation performed by Bowman, Hultberg and Martin[7] where they measured pressures on the tail and aft fuselage on a model spun in the wind tunnel. They found that the fuselage area on the outside under the horizontal tail contributes damping.

The tufts on top of the horizontal stabiliser indicate the presence of a leading edge vortex with rotation centre parallel to the leading edge. The second row (from the leading edge) of tufts on

https://doi.org/10.1017/S0001924000007028 Published online by Cambridge University Press

the inside stabilisator indicated reverse flow and on the outside stabilisator the flow was mainly spanwise outwards. This can be observed in Figs 18 and 22. Again, it is interesting to compare this experimental observation with the pressure measurements from the wind tunnel[7]. In the wind tunnel, the negative pressures were larger on top of the outside stabilisator than the inside. This might indicate that the vortex is generating a flow outwards, which result in more suction on the outside than the inside.

5.0 DISCUSSION AND CONCLUSIONS

Camera tracking the two-turn Slingsby spin has produced data and unique illustrations for analysis. This was possible due to CAD model creation using laser scanning and obtaining video and still imagery of unprecedented quality using a helicopter as chase aircraft. It was a challenge to track both the aeroplane and camera simultaneously. It is clear that the background points used in camera tracking are important in order to accurately establish the initial conditions. Other data sources, such as inertial or GPS position data from the camera, would have been helpful in the post processing of data. In the future it is hoped to use air-data measurements to validate and better quantify these methods for estimating alpha and beta.

The qualitative assessment of the airflow on the spinning Slingsby indicated that a vortex forms on the outside wing. This vortex, how it forms its movement on the wing, has been related to the spin motion and data from the camera tracking. It is hypothesised that this vortex and its movement is key to the balance of forces created by the spinning wing. Furthermore, it is likely that the turbulence observed on the empennage is partly from the vortex formed on the wing.

Qualitative assessment of the flow across the tail and aft fuselage has shown three dimensional effects and vorticity, including the presence of a leading edge vortex on top of the horizontal stabilisator. This is not in agreement with spin theories of the past, where the horizontal tail was believed to be the cause for the ‘blanketing’ of the vertical tail. Furthermore, using a two dimensional view, the assumed effect of the vertical tail in the spin were believed to be dependent on its geometry alone without considering other effects from the full aeroplane configuration.

It has been said earlier that to be able to understand aerodynamics one must try to ‘see’ the airflow. A corollary is that to understand high-angle of attack flight one must try to see the vortices. Based on the results so far, it is likely that spin prediction criteria based on simplistic two dimensional effects and localised flow phenomena will fail.

Future research will endeavour to investigate further the aerodynamic flow on wings, tail and aft fuselage in the spin. A finer grid for the tufts (more and smaller tufts) and the use of other flow visualisation methods (e.g. smoke) will be considered. The future research plan includes the use of high-speed cameras (300 frames per second) to study the tufts in higher fidelity and also to include other aeroplane models in the research project.

ACKNOWLEDGMENTS

The authors are grateful to Jonny Engelsvoll for camera operation and movie production, Photographer Torje Fanebust Aas and Helicopter Pilot Kristian Elvestad for their help in providing chase for the spinning Slingsby. The authors also wish to thank Ricardo Ferreira for help with laser scanning and the creation of the CAD model, and Håvard Finnesand at VisCo AS for help with the 3D illustrations and camera tracking.

https://doi.org/10.1017/S0001924000007028 Published online by Cambridge University Press

REFERENCES

1. NEUMANN, H. Drooped leading edge, Flight test evaluation with a small general aviation airplane, 2006, SETP European Symposium, Dresden, Germany.
2. PHILIPP, H. Bailout during spin tests, 2006, SETP European Symposium, Dresden, Germany.
3. Defence Standard 00-970 Part 1, Section 3, Issue 2, Leaflet 18, *Spinning and Spin Recovery, Design Criteria for Spin Resistance and Spin Recovery*, December 1999.
4. FINN, E. Analysis of routine tests of monoplanes in the Royal Aircraft Establishment Free Spinning Tunnel, June 1937, Report No BA 1409.
5. BOWMAN, J.S. Summary of spin technology as related to light general-aviation airplanes, December 1971, NASA TN D-6575, Washington, DC, USA.
6. BURK, S.M., BOWMAN, J.S. and WHITE, W.L. Spin-tunnel investigation of the spinning characteristics of typical single-engine general aviation airplane designs. I — Low-wing model A: Effects of tail configurations, September 1977, NASA Technical Paper 1009.
7. BOWMAN, J.S., HULTBERG, R.S. and MARTIN, C.A. Measurements of pressures on the tail and aft fuselage of an airplane model during rotary motions at spin attitudes, 1989, NASA Technical Paper 2939.
8. STEWART, E.C., SUIT, W.T., MOUL, T.M. and BROWN, P.W. Spin tests of a single-engine, high-wing light airplane, January 1982, NASA Technical Paper 1927, Langley Research Center, Hampton, VA, USA.
9. STOUGH H.P., PATTON, J.M. and SLIWA, S.M. Flight investigation of the effect of tail configuration on stall, spin, and recovery characteristics of a low-wing general aviation research airplane, October 1986, NASA Technical Paper 2644, Langley, VA, USA.
10. STOUGH, H.P., DICARLO, D.J. and PATTON, J.M. Flight investigation of stall, spin, and recovery characteristics of a low-wing, single-engine T-tail light airplane, October 1985, NASA Technical Paper 2427, Langley VA, USA.
11. ENGLERT, S. Lancair Columbia 400 Spin Recovery Testing, 2005, SETP Symposium, LA, USA.
12. The Slingsby T67M200 Pilots Notes, incorporating the CAA approved flight manual, August 1985, Slingsby Aviation, UK.
13. Leica HDS 6000 Scanner, http://hds.leica-geosystems.com/en/HDS-Laser-Scanners-SW_5570.htm (Retrieved 11/01/11).
14. Leica Cyclone 6.0, http://hds.leica-geosystems.com/en/Leica-Cyclone_6515.htm (Retrieved 11/01/11).
15. 3Dreshaper 5.2, http://www.3dreshaper.com/en1/En_PointCloudProcess.htm (Retrieved 11/01/11).
16. Panasonic, Operating Instructions, Memory card Camera-Recorder, Model No AG-HPX500, DVCProHD, 2007, Matsushita Electric Industrial Co.
17. Kenyon Laboratories, http://www.ken-lab.com/stabilizers.html (Retrieved 21/11/11).
18. Pentax, SLR Digital Camera, K20D, 2008, Operating Manual, Pentax Corporation.
19. SynthEyes 64-Bit Version 2008.1.1028, 2009 Andersson Technologies.
20. Autodesk 3ds Max 2011, 2010, Autodesk.
21. JONES, B.M. and HASLAM, J.A.G. Airflow about stalled and spinning aeroplanes shown by cinematographic records of the movements of wool-tufts, August 1932, Aeronautical Research Committee, T.3291.
22. BROWN, A.P., DILLON, J., CRAIG, G. and ERDOS, R. Flight manoeuvre and spin characteristics of the Harvard Mk 4: Application to human factors flight research, 16-19 August 2004, AIAA Atmospheric Flight Mechanics Conference and Exhibition, Providence, Rhode Island, 2004-4815.
23. Sony, Handycam HDR-CX105, 2009, Sony Corporation.
24. JVC Everio G, Hard Disk Camcorder, GZ-MG840BE, HDD, 2008, Victor Company of Japan.
25. Muvi Micro DV Camcorder, http://www.veho-uk.com/main/index.aspx (Retrieved 7/02/11).

https://doi.org/10.1017/S0001924000007028 Published online by Cambridge University Press